

COVER PAGE

Document downloaded by @DAEL

Sun Nov 29 00:58:44 2026
For personal use

When automatic English translation is provided, only the original document is authentic.
The EAA cannot be held responsible of any translation error

Bibliographical reference

Circumferential Waves in Piezoelectric Cylindrical Curved Plate, Jiangong Yu and Qiujuan Ma, Acta Acustica **vol. 94** (Number 5), 2008, pp. 725-733

DOI
https://doi.org/10.3813/AAA.918089

ACTA ACUSTICA UNITED WITH ACUSTICA
Vol. 94 (2008) 725 – 733

DOI 10.3813/AAA.918089

Circumferential Waves in Piezoelectric Cylindrical Curved Plate

Jiangong Yu
School of Mechanical and Power Engineering, Henan Polytechnic University, Jiaozuo 454003, P.R. China. yu@emails.bjut.edu.cn

Qiujuan Ma
College of Water Conservancy and Hydroelectric, Hebei University of Engineering, Handan 056021, P.R. China

Summary
Based on linear three-dimensional piezoelasticity, an orthogonal polynomial series expansion approach is used to determine the characteristics of guided circumferential waves in homogeneous anisotropic piezoelectric cylindrical curved plates. The displacement components and electrical potential, expanded in a series of Legendre polynomials, are introduced into the governing equations along with position-dependent material constants, so that the solution of the wave equation is reduced to an eigenvalue problem. The dispersion curves for PZT-4 and $Ba_2NaNb_5O_{15}$ cylindrical curved plates are calculated. The effect of piezoelectricity is also shown. Mechanical displacement distribution and electric potential distribution are illustrated and the influence of the radius to thickness ratio on the circumferential wave characteristics is discussed. Finally, the influence of the polarizing direction on the piezoelectric effect is shown.

PACS no. 43.20.Hq, 43.20.Bi

1. Introduction

Acoustic devices are widely used in the fields of electrical engineering, mechanical engineering and communications. Piezoelectric materials (PEM) are widely used for fabricating these acoustic devices. So far, PEM have been used, not only as small components in electro-mechanical Devices, but also as integrated structural elements [1]. The behaviour of the operational wave mode selected directly affects the performance of the device. Thus, a study of the wave characteristics in piezoelectric materials is an important part of the design procedure.

Many researchers have studied the vibration characteristics of cylinders and there is a considerable body of literature on the subject. There are two different groups of behaviour associated with waves in piezoelectric cylinders. One group is concerned with the waves propagating in the axial direction of a cylinder. Ambardar and Ferris [2] studied the wave propagation in a piezoelectric two-layered cylindrical shell with hexagonal symmetry. Srinivasamoorthy and Anandam [3] investigated the torsional wave propagation in an infinite piezoelectric 622 crystal glass cylinder. Paul and Raju used an asymptotic method developed by Achenbach to analyze the torsional [4] and longitudinal [5] modes of wave propagation in a piezoelectric solid circular cylinder of 6mm crystal glass. Using the same method, Paul and Venkatesan studied the axi-symmetric vibration of a piezoelectric solid cylinder coated by a thin film [6] and the wave propagation in a piezoelectric hollow cylinder of glass (6-mm) crystals [7]. Paul and Venkatesan also used the Fourier expansion collocation method to investigate the wave propagation in a piezoelectric solid cylinder of arbitrary cross section [8], in a piezoelectric solid cylinder of arbitrary cross section with a circular cylindrical cavity [9], in a piezoelectric human bone of arbitrary cross section with a circular cylindrical cavity [10] and in a piezoelectric bone with a cylindrical cavity of arbitrary shape [11]. Wang studied axial symmetric waves in piezoelectric coupled cylindrical shells, using the basic membrane shell model [12], and axial symmetric waves in piezoelectric coupled cylindrical shells with bending resistance, using a shell bending model under the inherent shear-rigidity assumption [13]. By employing both the separation of variables and the interpolation techniques, Ding *et al.* [14] investigated the axi-symmetric plane strain electro-elastic dynamic behaviour of hollow cylinders.

Another behaviour group is concerned with the waves circulating in the circumferential direction. Chen [15] studied the axial polarized shear waves travelling around the periphery of a piezoelectric cylinder of hexagonal crystal symmetry. Sun and Cheng [16] were concerned with the propagation of axially polarized shear waves circulating around a piezoelectric 6mm cylinder covered with a conducting layer. However, circumferential waves in elastic cylinders have received much attention. Different aspects of circumferential wave propagation along one or

Received 11 August 2006,
accepted 3 January 2008.

© S. Hirzel Verlag · EAA

multiple curved surfaces have been analyzed by Grace and Goodman [17], Qu and Berthelot [18], Cerv [19], Liu and Qu [20, 21] and Valle, Qu, and Jacobs [22] and He and Li [23] in isotropic elastic material. Also, Towfighi *et al.* [24] and Yu *et al.* [25] have studied circumferential wave propagation in anisotropic cylindrical curved plates.

The objective of this paper is to present an analysis of circumferential wave motion in anisotropic piezoelectric cylindrical curved plates by the Legendre orthogonal polynomial series expansion method, which was developed by Lefebvre *et al.* [26] to analyse free-ultrasonic waves in multi-layered plates. Guided wave dispersion curves for PZT-4 and $Ba_2NaNb_5O_{15}$ cylindrical curved plates as well as the corresponding non-piezoelectric cylindrical curved plates are calculated to show the effect of piezoelectricity. Mechanical displacement distribution and electric potential distribution are also illustrated. Guided wave dispersion curves for different ratios of radius to thickness are calculated and the resultant influence of this ratio on the wave characteristics is discussed. The influence of the polarizing direction on the piezoelectric effect is shown. In this paper, the open circuit surface is assumed.

2. Mathematics and formulation of the problem

Based on linear three-dimensional piezoelasticity, consider an anisotropic piezoelectric hollow cylinder. Let a, b, h be the inner, outer radius and the thickness, respectively. The linear constitutive relations of a cylindrical anisotropic piezoelectric medium are

$$\begin{Bmatrix} T_{\theta\theta} \\ T_{xx} \\ T_{rr} \\ T_{zz} \\ T_{r\theta} \\ T_{\theta z} \end{Bmatrix} = \begin{bmatrix} C_{11} & C_{12} & C_{13} & C_{14} & C_{15} & C_{16} \\ & C_{22} & C_{23} & C_{24} & C_{25} & C_{26} \\ & & C_{33} & C_{34} & C_{35} & C_{36} \\ & & & C_{44} & C_{45} & C_{46} \\ & \text{symmetry} & & & C_{55} & C_{56} \\ & & & & & C_{66} \end{bmatrix} \begin{Bmatrix} \varepsilon_{\theta\theta} \\ \varepsilon_{zz} \\ \varepsilon_{rr} \\ 2\varepsilon_{rz} \\ 2\varepsilon_{r\theta} \\ 2\varepsilon_{\theta z} \end{Bmatrix} - \begin{bmatrix} e_{11} & e_{21} & e_{31} \\ e_{12} & e_{22} & e_{32} \\ e_{13} & e_{23} & e_{33} \\ e_{14} & e_{24} & e_{34} \\ e_{15} & e_{25} & e_{35} \\ e_{16} & e_{26} & e_{36} \end{bmatrix} \begin{Bmatrix} E_\theta \\ E_z \\ E_y \end{Bmatrix}, \tag{1a}$$

$$\begin{Bmatrix} D_\theta \\ D_z \\ D_r \end{Bmatrix} = \begin{bmatrix} e_{11} & e_{12} & e_{13} & e_{14} & e_{15} & e_{16} \\ e_{21} & e_{22} & e_{23} & e_{24} & e_{25} & e_{26} \\ e_{31} & e_{32} & e_{33} & e_{34} & e_{35} & e_{36} \end{bmatrix} \begin{Bmatrix} \varepsilon_{\theta\theta} \\ \varepsilon_{zz} \\ \varepsilon_{rr} \\ 2\varepsilon_{rz} \\ 2\varepsilon_{r\theta} \\ 2\varepsilon_{\theta z} \end{Bmatrix} + \begin{bmatrix} \in_{11} & \in_{12} & \in_{13} \\ & \in_{22} & \in_{23} \\ \text{symm.} & & \in_{33} \end{bmatrix} \begin{Bmatrix} E_\theta \\ E_z \\ E_r \end{Bmatrix}. \tag{1b}$$

Generalized geometric equations in cylindrical co-ordinates are

$$\varepsilon_{\theta\theta} = \frac{1}{r}\frac{\partial u_r}{\partial r} + \frac{u_r}{r}, \qquad \varepsilon_{zz} = \frac{\partial u_z}{\partial z}, \qquad \varepsilon_{rr} = \frac{\partial u_r}{\partial r},$$

$$\varepsilon_{r\theta} = \Big(\frac{1}{r}\frac{\partial u_r}{\partial \theta} + \frac{\partial u_\theta}{\partial r} - \frac{u_\theta}{r}\Big), \quad \varepsilon_{rz} = \frac{1}{2}\Big(\frac{\partial u_r}{\partial z} + \frac{\partial u_z}{\partial r}\Big),$$
$$\varepsilon_{\theta z} = \frac{1}{2}\Big(\frac{\partial u_\theta}{\partial z} + \frac{\partial u_z}{r\partial \theta}\Big), \tag{2}$$
$$E_\theta = -\frac{1}{r}\frac{\partial \Phi}{\partial \theta}, \qquad E_z = -\frac{\partial \Phi}{\partial z}, \qquad E_r = -\frac{\partial \Phi}{\partial r}.$$

And the field equations governing wave propagation are

$$\begin{aligned} \frac{\partial T_{rr}}{\partial r} + \frac{1}{r}\frac{\partial T_{r\theta}}{\partial \theta} + \frac{\partial T_{rz}}{\partial z} + \frac{T_{rr} - T_{\theta\theta}}{r} &= \rho\frac{\partial^2 u_r}{\partial t^2}, \\ \frac{\partial T_{r\theta}}{\partial r} + \frac{1}{r}\frac{\partial T_{\theta\theta}}{\partial \theta} + \frac{\partial T_{\theta z}}{\partial z} + \frac{2T_{r\theta}}{r} &= \rho\frac{\partial^2 u_\theta}{\partial t^2}, \\ \frac{\partial T_{rz}}{\partial r} + \frac{1}{r}\frac{\partial T_{\theta z}}{\partial \theta} + \frac{\partial T_{zz}}{\partial z} + \frac{T_{rz}}{r} &= \rho\frac{\partial^2 u_z}{\partial t^2}, \\ \frac{\partial D_r}{\partial r} + \frac{1}{r}\frac{\partial D_\theta}{\partial \theta} + \frac{\partial D_z}{\partial z} + \frac{D_r}{r} &= 0, \end{aligned} \tag{3}$$

where T_{ij} and ε_{ij} are the stress and strain tensors; Φ and D_i are the electric potential and electric displacement vectors; C_{ij}, $\in_{ij}$ and e_{ij} are the elastic, dielectric and piezoelectric constants; ρ is the mass density.

Considering the boundary of the PEM with an open circuit surface, the position dependence of the elastic, dielectric, piezoelectric constants and mass density are given by

$$\begin{aligned} C(r) &= C\pi(r), \quad \rho(r) = \rho\pi(r), \\ e(r) &= e\pi(r), \quad \in(r) = \in \pi(r), \end{aligned} \tag{4}$$

where $\pi(r)$ is the rectangular window function defined by

$$\pi(r) = \begin{cases} 1, & a \le r \le b, \\ 0, & \text{elsewhere.} \end{cases}$$

Given equation (4), the material constants vanish outside the material. Thus, the vacuum outside the material is defined as a medium with zero acoustic impedance and zero electric displacement, which ensures that $T_{rr} = T_{rz} = T_{r\theta} = 0$ and $D_r = 0$ when $r = a$, $r = b$.

For a free harmonic wave propagating in the circumferential direction in a circular cylinder of infinite length, it can be assumed that the displacement components are of the form

$$u_r(r, \theta, z, t) = \exp\big(\mathrm{i}kb\theta - \mathrm{i}\omega t\big)U(r), \tag{5a}$$
$$u_\theta(r, \theta, z, t) = \exp\big(\mathrm{i}kb\theta - \mathrm{i}\omega t\big)V(r), \tag{5b}$$
$$u_z(r, \theta, z, t) = \exp\big(\mathrm{i}kb\theta - \mathrm{i}\omega t\big)W(r), \tag{5c}$$
$$\Phi(r, \theta, z, t) = \exp\big(\mathrm{i}kb\theta - \mathrm{i}\omega t\big)X(r), \tag{5d}$$

$U(r)$, $V(r)$, $W(r)$ represent the amplitude of vibration in the radial, circumferential and axial directions, respectively, and $X(r)$ represents the amplitude of electric potential. k is the magnitude of the wave vector in the propagation direction, and ω the angular frequency.

Substituting equations (1), (2), (4), (5) into equation (3), the governing differential equations in terms of displacement and electric potential components can be obtained,

$$
\begin{aligned}
&\{r^2(C_{33}U'' + C_{35}V'' + C_{34}W'' + C_{33}X'')\\
&+ r(C_{33} + 2ikbC_{35})U' + r\big[ikb(C_{13} + C_{55}) - C_{15}\big]V'\\
&+ r\big[(C_{34} + C_{14}) + ikb(C_{36} + C_{45})\big]W'\\
&+ r\big[e_{33} - e_{31} + ikb(e_{13} + e_{35})\big]X' - r(k^2b^2C_{55} + C_{11})U\\
&\big[C_{15} - k^2b^2C_{15} - ikb(C_{55} + C_{11})\big]V\\
&- \big[k^2b^2C_{56} + ikbC_{16}\big]W\\
&+ \big[ikb(e_{13} - e_{11}) - k^2b^2e_{15}\big]X\}\pi(r)\\
&+ \big(\delta(r-a) - \delta(r-b)\big)\\
&\quad\cdot\{r^2(C_{33}U' + C_{35}V' + C_{34}W' + e_{33}X')\\
&\qquad + r\big[(C_{13} + ikbC_{35})U + r(ikbC_{35} - C_{35})V\\
&\qquad + ikbC_{36}W + ikbe_{13}X\big]\} = -\rho r^2\omega^2 U\pi(r), \qquad (6a)
\end{aligned}
$$

$$
\begin{aligned}
&\{r^2(C_{35}U'' + C_{55}V'' + C_{45}W'' + C_{35}X'')\\
&+ r\big[2C_{35} + C_{15} + ikb(C_{13} + C_{55})\big]U'\\
&+ r(C_{55} + 2ikbC_{15})V' + r\big[2C_{45} + ikb(C_{14} + C_{56})\big]W'\\
&+ r\big[ikb(e_{31} + e_{15}) + 2e_{35}\big]X'\\
&+ \big[ikb(C_{55} + C_{11}) - k^2b^2C_{15} + C_{15}\big]U\\
&- (C_{55} + k^2b^2C_{11})V + (ikbC_{56} - k^2b^2C_{16})W\\
&+ (2ikbe_{15} - k^2b^2e_{11})X\}\pi(r)\\
&+ \big(\delta(r-a) - \delta(r-b)\big)\\
&\quad\cdot\{r^2(C_{35}U' + C_{55}V' + C_{45}W' + e_{35}X')\\
&\qquad + r(C_{15} + ikbC_{55})U + r(ikbC_{15} - C_{55})V\\
&\qquad + r(ikbC_{15} - C_{55})W\\
&\qquad + rikbC_{56}W + rikbe_{15}X\big]\} = -\rho r^2\omega^2 V\pi(r), \qquad (6b)
\end{aligned}
$$

$$
\begin{aligned}
&\{r^2(C_{34}U'' + C_{45}V'' + C_{44}W'' + C_{34}X'')\\
&+ r\big[C_{34} + C_{14} + ikb(C_{36} + C_{45})\big]U'\\
&+ rikb(C_{14} + C_{56})V' + r(C_{44} + 2ikbC_{46})W'\\
&+ r\big[ikb(e_{36} + e_{14}) + e_{34}\big]X' + (ikbC_{16} - k^2b^2C_{56})U\\
&- (ikbC_{56} + k^2b^2C_{16})V - k^2b^2C_{66}W\\
&- k^2b^2e_{16})X\}\pi(r) + \big(\delta(r-a) - \delta(r-b)\big)\\
&\quad\cdot\{r^2(C_{34}U' + C_{45}V' + C_{44}W' + e_{34}X')\\
&\qquad + r(C_{14} + ikbC_{45})U + r(ikbC_{14} - C_{45})V\\
&\qquad + rikbC_{46}W + rikbe_{14}X\big]\} = -\rho r^2\omega^2 W\pi(r), \qquad (6c)
\end{aligned}
$$

$$
\begin{aligned}
&\{r^2(C_{33}U'' + C_{35}V'' + C_{34}W'' + C_{33}X'')\\
&+ r\big[e_{31} + e_{33} + ikb(e_{13} + e_{35})\big]U'\\
&+ rikb(e_{31} + e_{15})V' + r\big[ikb(e_{36} - e_{14}) + e_{34}\big]W'\\
&- r\big[\in_{33} + 2ikb\in_{13}\big]X' + (ikbe_{11} - k^2b^2e_{15})U\\
&- (ikbe_{15} + k^2b^2e_{11})V - k^2b^2e_{16}W\\
&- ikb\in_{13} + k^2b^2\in_{11})X\}\pi(r)\\
&+ \big(\delta(r-a) - \delta(r-b)\big)\{r^2(e_{31}U' + ikbe_{35})U\\
&\qquad + r(ikbe_{31} - e_{35})V + ikbe_{36}W - rikb\in_{13} X\\
&\qquad + r^2(e_{33}U' + e_{35}V' + e_{34}W' - e_{33}X')\} = 0, \qquad (6d)
\end{aligned}
$$

where, $U(r)$, $V(r)$, $W(r)$ and $X(r)$ can be expanded in a Legendre orthogonal polynomial series as

$$
\begin{aligned}
U(r) &= \sum_{m=0}^{\infty} p_m^1 Q_m(r), \qquad V(r) = \sum_{m=0}^{\infty} p_m^2 Q_m(r),\\
W(r) &= \sum_{m=0}^{\infty} p_m^3 Q_m(r), \qquad X(r) = \sum_{m=0}^{\infty} r_m Q_m(r) \qquad (7)
\end{aligned}
$$

where p_m^i $(i = 1, 2, 3)$ and r_m is the expansion coefficient and

$$
Q_m(r) = \sqrt{\frac{2m+1}{b-a}}\, P_m\Big(\frac{2r - (b+a)}{b-a}\Big),
$$

with P_m being the mth Legendre polynomial. Theoretically, m varies from 0 to ∞. In practice, each summation over the polynomials in equation (7) is truncated at some finite value $m = M$, when higher order terms become essentially negligible.

Multiplying $Q_j^*(r)$ with j varying from 0 to M, integrating over r from a to b, and taking advantage of the orthonormality of the functions, gives the following equations,

$$
\begin{aligned}
A_{11}^{j,m} p_m^1 + A_{12}^{j,m} p_m^2 + A_{13}^{j,m} p_m^3 + A_{14}^{j,m} r_m &= -\omega^2 N_m^j p_m^1, \qquad (8a)\\
A_{21}^{j,m} p_m^1 + A_{22}^{j,m} p_m^2 + A_{23}^{j,m} p_m^3 + A_{24}^{j,m} r_m &= -\omega^2 N_m^j p_m^2, \qquad (8b)\\
A_{31}^{j,m} p_m^1 + A_{32}^{j,m} p_m^2 + A_{33}^{j,m} p_m^3 + A_{34}^{j,m} r_m &= -\omega^2 N_m^j p_m^3, \qquad (8c)\\
A_{41}^{j,m} p_m^1 + A_{42}^{j,m} p_m^2 + A_{43}^{j,m} p_m^3 + A_{44}^{j,m} r_m &= 0, \qquad (8d)
\end{aligned}
$$

where $A_{\alpha\beta}^{j,m}$ $(\alpha, \beta = 1, 2, 3, 4)$ and M_m^j are the elements of a non-symmetric matrix, which can be obtained from equation (6).

Equation (8d) can be written as:

$$
r_m = -\big(A_{44}^{j,m}\big)^{-1}\big(A_{41}^{j,m} p_m^1 + A_{42}^{j,m} p_m^2 + A_{43}^{j,m} p_m^3\big). \qquad (9)
$$

Substituting equation (9) into equations (8a), (8b), (8c) yields

$$
\begin{aligned}
&\big[A_{11}^{j,m} - A_{14}^{j,m}(A_{44})^{-1}A_{41}^{j,m}\big]p_m^1\\
&+ \big[A_{12}^{j,m} - A_{14}^{j,m}(A_{44})^{-1}A_{42}^{j,m}\big]p_m^2 \qquad (10a)\\
&+ \big[A_{13}^{j,m} - A_{14}^{j,m}(A_{44})^{-1}A_{43}^{j,m}\big]p_m^3 = -\omega^2 M_m^j p_m^1,\\
&\big[A_{21}^{j,m} - A_{24}^{j,m}(A_{44})^{-1}A_{41}^{j,m}\big]p_m^1\\
&+ \big[A_{22}^{j,m} - A_{24}^{j,m}(A_{44})^{-1}A_{42}^{j,m}\big]p_m^2 \qquad (10b)\\
&+ \big[A_{23}^{j,m} - A_{24}^{j,m}(A_{44})^{-1}A_{43}^{j,m}\big]p_m^3 = -\omega^2 M_m^j p_m^2,\\
&\big[A_{31}^{j,m} - A_{34}^{j,m}(A_{44})^{-1}A_{41}^{j,m}\big]p_m^1\\
&+ \big[A_{32}^{j,m} - A_{34}^{j,m}(A_{44})^{-1}A_{42}^{j,m}\big]p_m^2 \qquad (10c)\\
&+ \big[A_{33}^{j,m} - A_{34}^{j,m}(A_{44})^{-1}A_{43}^{j,m}\big]p_m^3 = -\omega^2 M_m^j p_m^3.
\end{aligned}
$$

Equation (10) can be written as

$$
\begin{aligned}
&\begin{bmatrix} \overline{A}_{11}^{j,m} & \overline{A}_{12}^{j,m} & \overline{A}_{13}^{j,m} \\ \overline{A}_{21}^{j,m} & \overline{A}_{22}^{j,m} & \overline{A}_{22}^{j,m} \\ \overline{A}_{31}^{j,m} & \overline{A}_{32}^{j,m} & \overline{A}_{33}^{j,m} \end{bmatrix} \begin{Bmatrix} p_m^1 \\ p_m^2 \\ p_m^3 \end{Bmatrix}\\
&= -\omega^2 \begin{bmatrix} M_m^j & 0 & 0 \\ 0 & M_m^j & 0 \\ 0 & 0 & M_m^j \end{bmatrix} \begin{Bmatrix} p_m^1 \\ p_m^2 \\ p_m^3 \end{Bmatrix}. \qquad (11)
\end{aligned}
$$

The solution of equation (11) is that of an eigenvalue problem. The eigenvalue ω^2 gives the angular frequency of the guided wave; eigenvectors p_m^i ($i = 1, 2, 3$) enable the components of the particle displacement to be calculated; and r_m, which can be obtained from equation (9), determines the electric potential. According to $Vph = \omega/k$ and $Vg = \mathrm{d}\omega/\mathrm{d}k$, the phase velocity and group velocity can be obtained. The complex matrix equation (11) can be solved numerically making use of standard computer programs for the diagonalization of non-symmetric square matrices. In practice the summations over the polynomials for the $3(M + 1)$ eigenmodes are generated from the order M of the expansion. Acceptable solutions are those eigenmodes for which convergence is obtained as M is increased. The point at which the eigenvalues obtained could be considered converged solutions was when a further increase in the matrix dimension did not result in a significant change in the eigenvalue. The computer program was written using Mathmatica.

When the material is orthotropic or has fewer independent constants in the wave propagation direction, and is polarized in the radial direction, the governing differential equations are reduced to

$$\begin{aligned}&\big\{r^2(C_{33}U'' + e_{33}X'') + rC_{33}U' + rikb(C_{13} + C_{55})V'\\&+ r(e_{33} - e_{31})X' - (k^2b^2C_{55} + C_{11})U\\&- ikb(C_{55} + C_{11})\big]V - k^2b^2e_{15}X\big\}\pi(r)\\&+ \big(\delta(r-a) - \delta(r-b)\big)\big\{r^2(C_{33}U' + e_{33}X')\\&+ r(C_{13}U + ikbC_{13}V) = -\rho r^2\omega^2U\pi(r),\end{aligned} \tag{12a}$$

$$\begin{aligned}&\big\{r^2C_{55}V'' + rikb(C_{13} + C_{55})U' + rC_{55}V'\\&+ rikb(e_{31} + e_{15})X' + ikb(C_{55} + C_{11})U\\&- (C_{55} + k^2b^2C_{11})V + 2ikbe_{15}X\big\}\pi(r),\\&+ \big(\delta(r-a) - \delta(r-b)\big)\big(r^2C_{55}V' + rikbC_{55}U\\&- rC_{55}V + rikbe_{15}\big) = -\rho r^2\omega^2V\pi(r),\end{aligned} \tag{12b}$$

$$\begin{aligned}&\big(r^2C_{44}W'' + rC_{44}W' - k^2b^2C_{66}W\big)\pi(r)\\&+ \big(\delta(r-a) - \delta(r-b)\big)r^2C_{44}W' = -\rho r^2\omega^2W\pi(r),\end{aligned} \tag{12c}$$

$$\begin{aligned}&\big\{r^2(e_{33}U'' - \in_{33} X'') + r(e_{31} + e_{33})U'\\&+ rikb(e_{31} + e_{15})V' - r(\in_{33} + 2ikb \in_{13})X' + k^2b^2e_{15}U\\&- ikbe_{15}V + k^2b^2 \in_{11} X\big\}\pi(r) + \big(\delta(r-a) - \delta(r-b)\big)\\&\cdot \big(r^2(e_{33}U' - \in_{33} X') + re_{31}U + rikbe_{31}V\big) = 0.\end{aligned} \tag{12d}$$

Here, equation (12c) is independent of the other three equations, and equations (12a), (12b) and (12d) are coupled with each other. In fact, equation (12c) represents the propagating circumferential SH wave. It is not influenced by the piezoelectricity when the material is polarized in the radial direction, and it can be solved analytically. Equations (12a) and (12b) control the propagating Lamb-type waves. Apart from equation (12c), the Lamb-type waves governing the differential equations are reduced to

$$\begin{bmatrix} \overline{A'}_{11}^{j,m} & \overline{A'}_{13}^{j,m} \\ \overline{A'}_{31}^{j,m} & \overline{A'}_{33}^{j,m} \end{bmatrix} \begin{Bmatrix} p_m^{'1} \\ p_m^{'3} \end{Bmatrix} = -\eta^2 \begin{bmatrix} M_m^j & 0 \\ 0 & M_m^j \end{bmatrix} \begin{Bmatrix} p_m^{'1} \\ p_m^{'3} \end{Bmatrix}. \tag{13}$$

When the material is orthotropic and is polarized in the circumferential direction, the governing differential equations are

$$\begin{aligned}&\big\{r^2C_{33}U'' + rC_{33}U' + rikb(C_{13} + C_{55})V'\\&+ rikb(e_{13} + e_{35})X' - (k^2b^2C_{55} + C_{11})U\\&- ikb(C_{55} + C_{11})\big]V + ikb(e_{13} - e_{11})X\big\}\pi(r)\\&+ \big(\delta(r-a) - \delta(r-b)\big)\big(r^2C_{33}U' + rC_{13}U + ikbC_{13}V\\&+ rikbe_{13}X\big) = -\rho r^2\omega^2U\pi(r),\end{aligned} \tag{14a}$$

$$\begin{aligned}&\big\{r^2(C_{55}V'' + e_{35}X'') + rikb(C_{13} + C_{55})U' + rC_{55}V'\\&+ r2e_{35}X' + ikb(C_{55} + C_{11})U\\&- (C_{55} + k^2b^2C_{11})V - k^2b^2e_{11}X\big\}\pi(r),\\&+ \big(\delta(r-a) - \delta(r-b)\big)\big(r^2(C_{55}V' + e_{35}X') + rikbC_{55}U\\&- rC_{55}V\big) = -\rho r^2\omega^2V\pi(r),\end{aligned} \tag{14b}$$

$$\begin{aligned}&\big(r^2C_{44}W'' + rC_{44}W' - k^2b^2C_{66}W\big)\pi(r)\\&+ \big(\delta(r-a) - \delta(r-b)\big)r^2C_{44}W' = -\rho r^2\omega^2W\pi(r),\end{aligned} \tag{14c}$$

$$\begin{aligned}&\big\{r^2(e_{35}V'' - \in_{33} X'') + rikb(e_{13} + e_{35})U' - r \in_{33} X'\\&+ ikbe_1U - k^2b^2e_{11}V + k^2b^2 \in_{11} X\big\}\pi(r)\\&+ \big(\delta(r-a) - \delta(r-b)\big)\\&\cdot \big(rikbe_{35}U - re_{35}V + r^2(e_{35}V' - \in_{33} X')\big) = 0.\end{aligned} \tag{14d}$$

Similarly, the independent SH wave is not affected by the piezoelectricity.

3. Numerical results

Based on the foregoing formulations, a computer program has been written to calculate the circumferential wave dispersion curves of the PZT-4 and $Ba_2NaNb_5O_{15}$ cylindrical curved plates as well as the corresponding non-piezoelectric cylindrical curved plates. Their material constants with radial polarization are listed in Table I, and the other constants are all zero. The series expansions of equation (7) are truncated at $M = 10$ for all the following calculations.

Figures 1 and 2 show the circumferential Lamb-type wave frequency spectra and phase velocity spectra for PZT-4 and $Ba_2NaNb_5O_{15}$ cylindrical curved plates, and for the corresponding non-piezoelectric cylindrical curved plates with $a = 9$ mm and $b = 10$ mm. Whatever the material, for a definite mode, the phase velocities of PEM cylinders are larger than those of the corresponding non-piezoelectric cylinders and the piezoelectric effect becomes stronger as wave number increases. In micro-scale SAW devices, the operating frequency is usually very high and the wavelength is very small (i.e. large wave number). Therefore, the piezoelectric effects will be prominent.

Furthermore, it can be seen that the effect of piezoelectricity is stronger with PZT-4 than with $Ba_2NaNb_5O_{15}$.

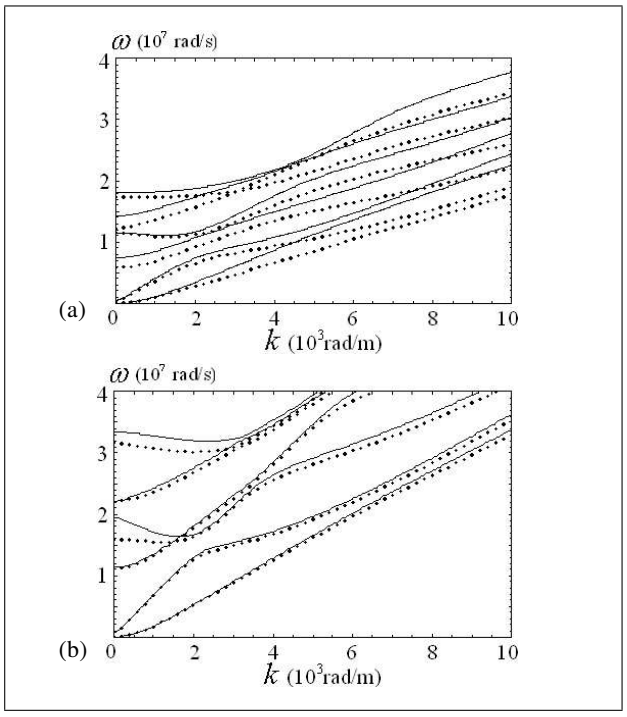

Figure 1. Frequency spectra for PEM cylindrical curved plates: solid line, piezoelectric; dotted line, non-piezoelectric, (a) PZT-4; (b) $Ba_2NaNb_5O_{15}$.

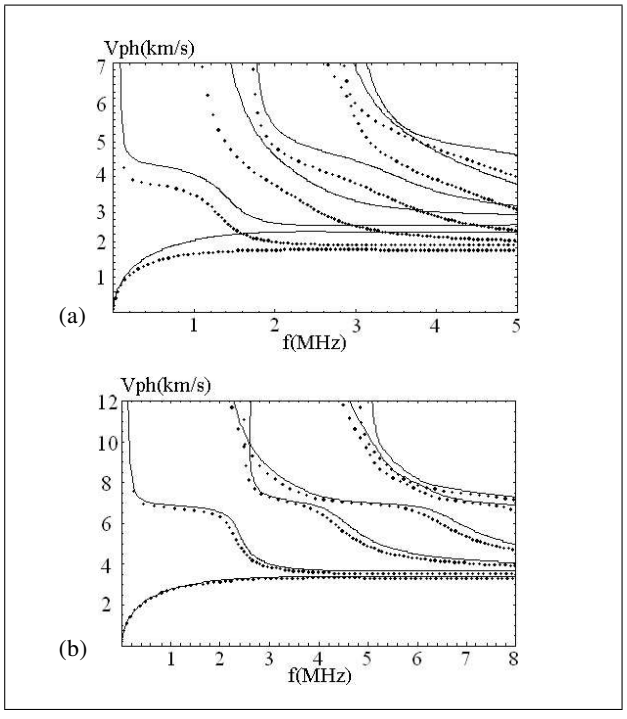

Figure 2. Phase velocity spectra for PEM cylindrical curved plates: solid line, piezoelectric; dotted line, non-piezoelectric, (a) PZT-4; (b) $Ba_2NaNb_5O_{15}$.

It is clear from equation (10), that the piezoelectric effect is related to the elastic constants, dielectric constants, and piezoelectric constants. When keeping the elastic constants invariable, the piezoelectric effect is directly proportional to the piezoelectric constants and is inversely proportional to the dielectric constants. When keeping the dielectric constants and piezoelectric constants invariable, the piezoelectric effect is inversely proportional to the elastic constants. Figures 3 and 4 verifies this conclusion. Figure 3 shows the Frequency spectra for PZT-4 cylindrical curved plates when the piezoelectric constants and dielectric constants are increased by 200%. It can be seen that increasing the piezoelectric constants strengthens the piezoelectric effect, but increasing the dielectric constants weakens the piezoelectric effect. Figure 4 shows the Frequency spectra for $Ba_2NaNb_5O_{15}$ cylindrical curved plates when the elastic constants are divided by six. Clearly, the piezoelectric effect is strengthened.

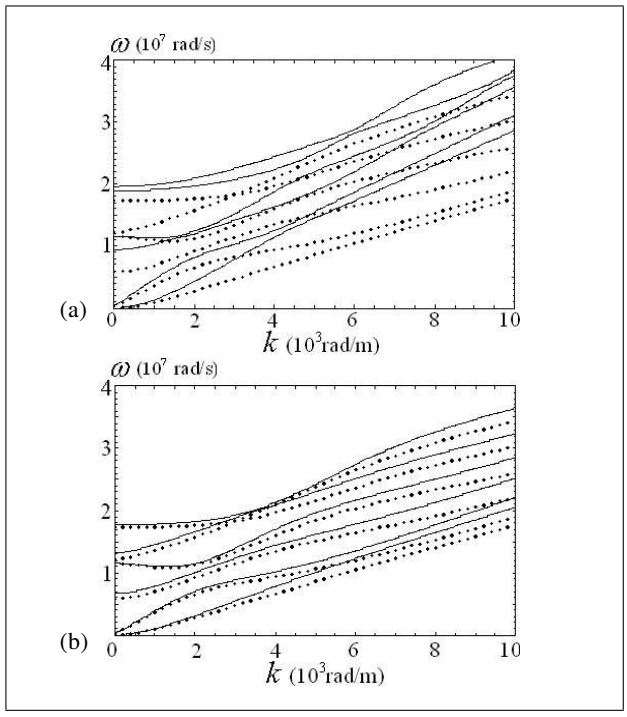

Figure 3. Frequency spectra for PZT-4 cylindrical curved plates: solid line, piezoelectric; dotted line, non-piezoelectric, (a) enlarge the piezoelectric constants; (b) enlarge the dielectric constants.

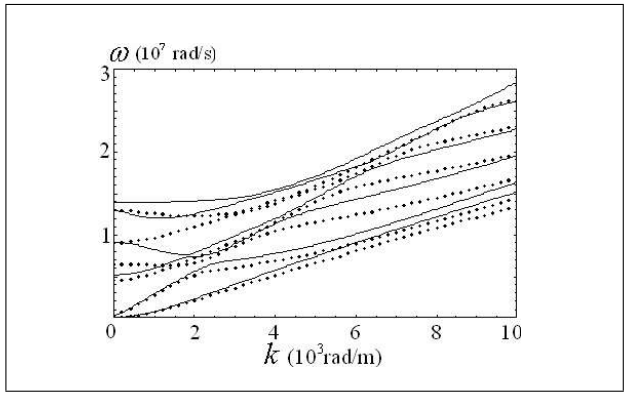

Figure 4. Frequency spectra for $Ba_2NaNb_5O_{15}$ cylindrical curved plates when decreasing the elastic constants: solid line, piezoelectric; dotted line, non-piezoelectric.

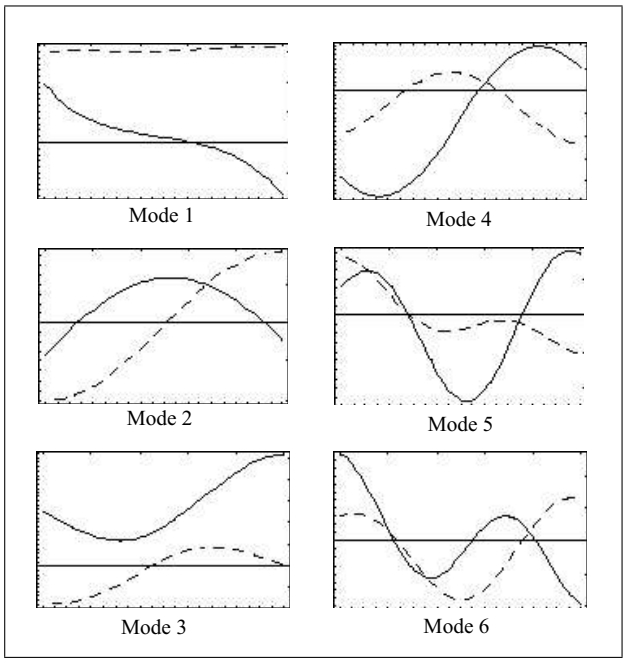

Figure 5. Mechanical displacement distribution in the thickness direction of $Ba_2NaNb_5O_{15}$ cylindrical curved plate (k = 3000 rad/m; dashed line u_r; solid line u_θ).

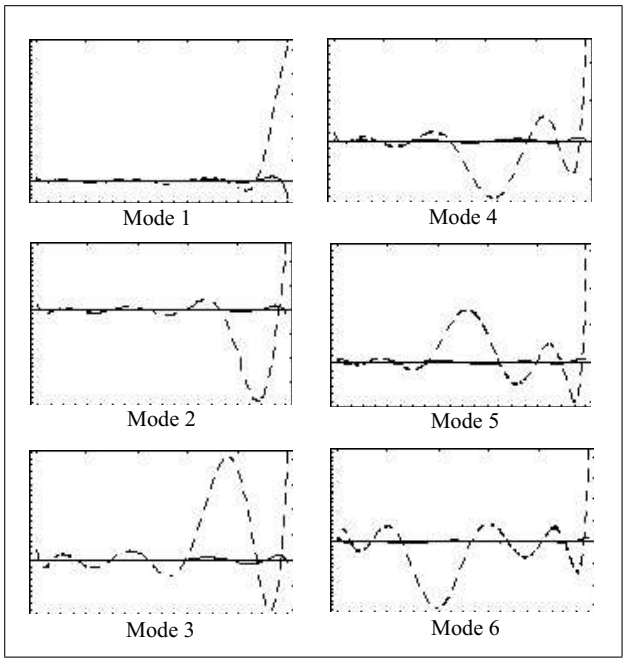

Figure 6. Mechanical displacement distribution in the thickness direction of $Ba_2NaNb_5O_{15}$ cylindrical curved plate (k = 300000 rad/m; dashed line u_r; solid line u_θ).

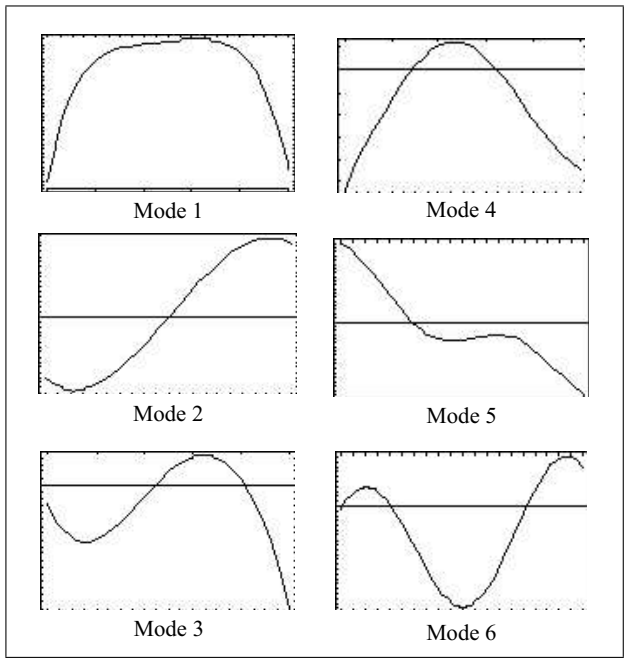

Figure 7. Electric potential distribution in the thickness direction of $Ba_2NaNb_5O_{15}$ cylindrical curved plate (k = 3000rad/m).

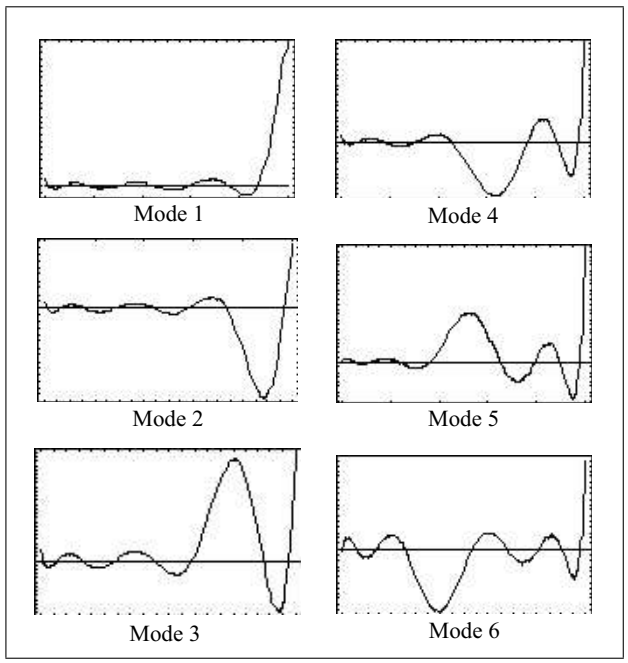

Figure 8. Electric potential distribution in the thickness direction of $Ba_2NaNb_5O_{15}$ cylindrical curved plate (k = 300000rad/m).

The displacement mode shapes and the electric potential distribution of the $Ba_2NaNb_5O_{15}$ cylindrical curved plate were investigated. Figures 5 and 6 show the 6 lowest displacement mode shapes of the piezoelectric cylindrical curved plate for k = 3000 and 300000 rad/m. It can be seen that for the larger wavenumber, the displacements of the 6 lowest modes in the piezoelectric cylindrical curved plate are mainly distributed in the neighbourhood of the outer surface. Figures 7 and 8 give the corresponding electrostatic potential modes for k = 3000 and 300000 rad/m, respectively. The phenomenon shown in these two figures is similar to that illustrated in Figures 5 and 6.

In order to investigate the effect of η (the ratio between the outer radius and thickness), the circumferential waves frequency spectra and group velocity spectra for $Ba_2NaNb_5O_{15}$ cylindrical curved plates are shown in

Table I. Material constants of two homogeneous piezoelectric materials. Units: C_{ij} (10^{10} N/m^2), $\in_{ij}$ (10^{-11} F/m^2), e_{ij} (C/m), ρ (10^3 kg/m^3).

Property	C_{11}	C_{12}	C_{13}	C_{22}	C_{23}	C_{33}	C_{44}	C_{55}	C_{66}
$Ba_2NaNb_5O_{15}$	23.9	10.4	5	24.7	5.2	13.5	6.5	6.6	7.6
PZT-4	13.9	7.8	7.4	13.9	7.4	11.5	2.56	2.56	3.05
	e_{15}	e_{24}	e_{31}	e_{32}	e_{33}	$\in_{11}$	$\in_{22}$	$\in_{33}$	ρ
$Ba_2NaNb_5O_{15}$	2.8	3.4	-0.4	-0.3	4.3	196	201	28	5.3
PZT-4	12.7	12.7	-5.2	-5.2	15.1	650	650	560	7.5

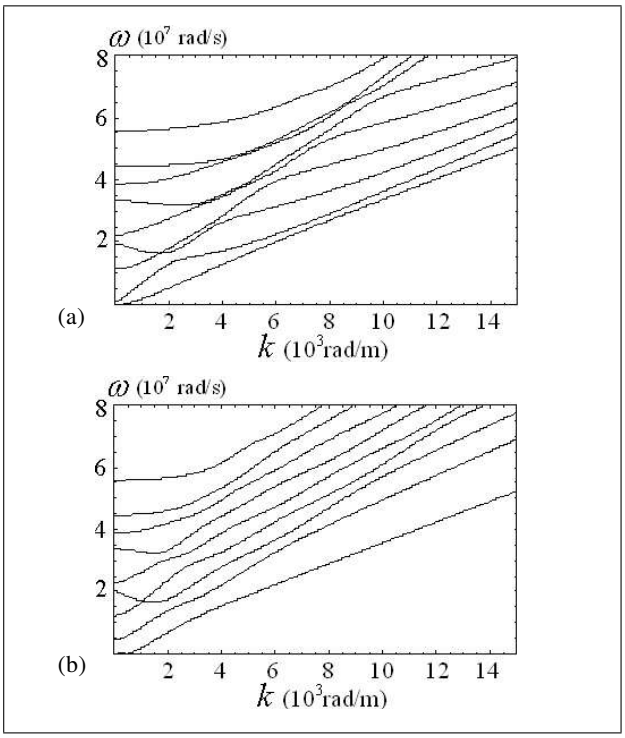

Figure 9. Dispersion relationships for $Ba_2NaNb_5O_{15}$ cylindrical curved plate, (a) $\eta = 10$, (b) $\eta = 2$.

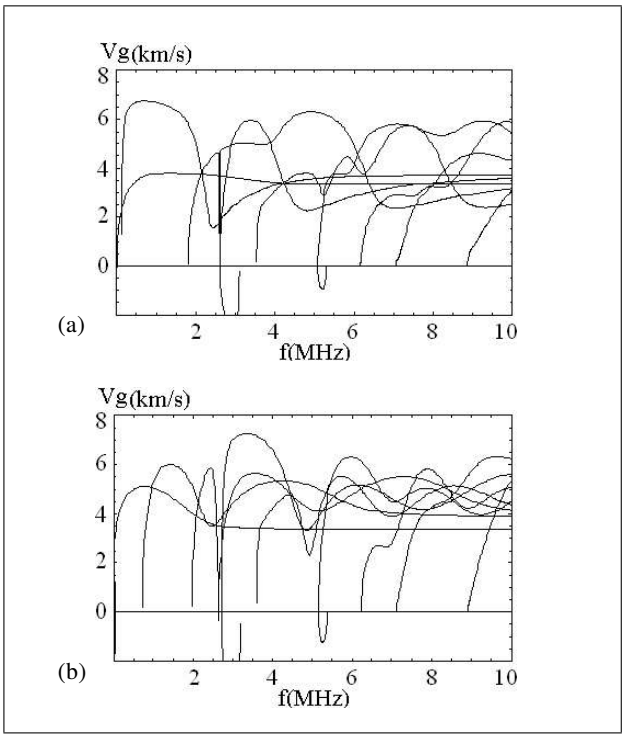

Figure 10. Group velocity dispersion curves for $Ba_2NaNb_5O_{15}$ cylindrical curved plate, (a) $\eta = 10$, (b) $\eta = 2$.

Figures 9 and 10. Here, b is 10 mm and 2 mm respectively but keeping $h = 1$ mm unchanged, i.e. $\eta = 10$ and 2. From Figure 9, it can be seen that the ratio of radius to thickness has considerable influence on the curves for all the modes, and that the larger the wavenumber, the stronger this effect. In addition, the effect is far stronger for lower order modes than for higher order modes when the wavenumber is small. From Figure 10, it can be seen that negative group velocity occurs at some modes regardless of the ratio. For the smaller η, the group velocity changes more sharply, and the group velocity maxima are larger, except for the second mode. The effect of η on the cut-off frequencies of lower modes is also clear, especially on the first cut-off frequency. The cut-off frequencies for the smaller η are higher than for the larger η.

Figure 11 gives the dispersion curves for the PZT-4 cylindrical curved Plate when polarization is in the circumferential direction. The geometrical size is the same as the structure of Figure 1(a). Under circumferential polarization, the piezoelectric and dielectric constants of PZT-4 are $e_{11} = e_{13} = -15.1$, $e_{12} = 5.2$, $e_{26} = e_{35} = -12.7$, $\in_{11}$= 560, $\in_{22}$=$\in_{33}$= 650. The elastic constants have been kept invariable to assist comparison. It can be seen that the piezoelectric effect is stronger for the higher order modes than for the lower order modes; the piezoelectric effect becomes weaker with increasing frequency and does not change much with wave number variation. This is significantly different from the radial polarization case. For radial polarization, the piezoelectric effect become stronger with increasing wave number and does not change much with varying frequency.

4. Conclusions

The Legendre orthogonal polynomial series expansion method is used to characterize the guided circumferen-

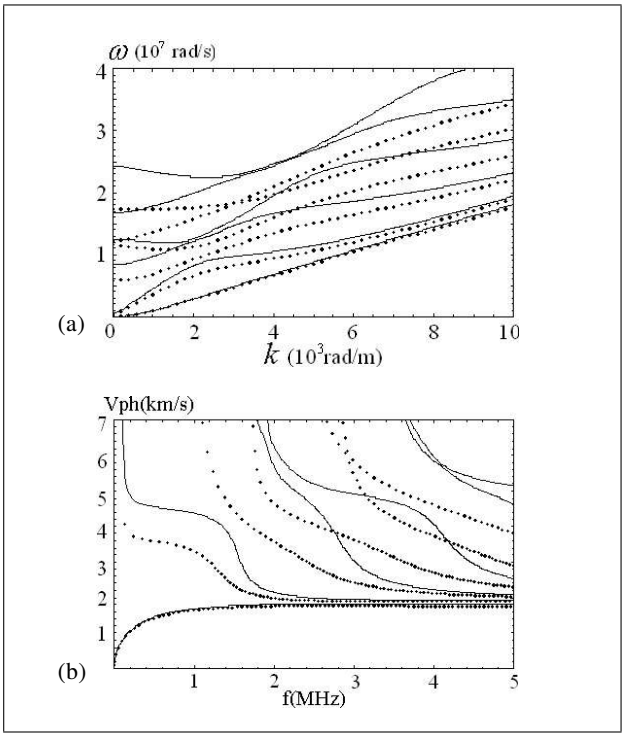

Figure 11. Dispersion curves for PZT-4 cylindrical curved plates with circumferential polarization: solid line, piezoelectric; dotted line, non-piezoelectric, (a) frequency spectra; (b) phase velocity spectra.

tial waves in anisotropic piezoelectric cylindrical curved plates. Guided wave dispersion curves, mechanical displacement distribution and electric potential distribution for PEM cylindrical curved plates are analyzed. Based on the calculated results, the following conclusions can be drawn:

1. For circumferential wave propagation in PEM cylindrical curved plates, the piezoelectric effect is directly proportional to the piezoelectric constants and is inversely proportional to the dielectric and elastic constants.
2. Mechanical displacements and electric potential are mainly distributed in the neighborhood of the outer surface when the wave number is large.
3. The ratio of radius to thickness has a significant influence on the characteristics of guided circumferential waves for the piezoelectric cylindrical curved plates.
4. The direction of polarization clearly influence the piezoelectric effect. For radial polarization, the piezoelectric effect is sensitive to wave number. For circumferential polarization, the piezoelectric effect is sensitive to frequency.

References

[1] S. S. Rao, M. Sunar: Piezoelectricity and its use in disturbance sensing and control of flexible structure: Survey. Appl. Mech. Rev. **47** (1994) 113–123.

[2] A. Ambardar, C. D. Ferris: Wave propagation in a piezoelectric two-layered cylindrical shell with hexagonal symmetry: Some implications for long bone. Journal of the Acoustical Society of America **63** (1978) 781–792.

[3] V. R. Srinivasamoorthy, C. Anandam: Torsional wave propagation in an infinite piezoelectric cylinder (622) crystal class. Journal of the Acoustical Society of America **67** (1980) 2034–2035.

[4] H. S. Paul, D. P. Raju: Asymptotic analysis of the torsional modes of wave propagation in a piezoelectric solid circular cylinder of (622) class. International Journal of Engineering Science **19** (1981) 1069–1076.

[5] H. S. Paul, D. P. Raju: Asymptotic analysis of the modes of wave propagation in a piezoelectric solid cylinder. Journal of the Acoustical Society of America **71** (1982) 255–263.

[6] H. S. Paul, M. Venkatesan: Axisymmetric vibration of a piezoelectric solid cylinder guided by a thin film. Journal of the Acoustical Society of America **80** (1986) 1091–1096.

[7] H. S. Paul, M. Venkatesan: Vibrations of a hollow circular cylinder of piezoelectric ceramics. Journal of the Acoustical Society of America **82** (1987) 952–956.

[8] H. S. Paul, M. Venkatesan: Wave propagation in a piezoelectric solid cylinder of arbitrary cross section. Journal of the Acoustical Society of America **82** (1987) 2013–2020.

[9] H. S. Paul, M. Venkatesan: Wave propagation in a piezoelectric ceramic cylinder of arbitrary cross section with a circular cylindrical cavity. Journal of the Acoustical Society of America **85** (1989) 163–170.

[10] H. S. Paul, M. Venkatesan: Wave propagation in a piezoelectric human bone of arbitrary cross section with a circular cylindrical cavity. Journal of the Acoustical Society of America **89** (1991) 196–199.

[11] H. S. Paul, M. Venkatesan: Wave propagation in a piezoelectric bone with a cylindrical cavity of arbitrary shape. International Journal of Engineering Science **29** (1991) 1601–1607.

[12] Q. Wang: Wave propagation in a piezoelectric coupled cylindrical membrane shell. International Journal of Solids and Structures **38** (2001) 8207–8218.

[13] Q. Wang: Axi-symmetric wave propagation in a cylinder coated with a piezoelectric layer. International Journal of Solids and Structures **39** (2002) 3023–3037.

[14] H. J. Ding, H. M. Wang, P. F. Hou: The transient responses of piezoelectric hollow cylinders for axisymmetric plane strain problems. International Journal of Solids and Structures **40** (2003) 105–123.

[15] C. L. Chen: On the electroacoustic waves guided by a cylindrical piezoelectric interface. J. Appl. Phys. **44** (1973) 3841–47.

[16] C. T. Sun, N. C. Cheng: Piezoelectric waves on a layered cylinder. J. Appl. Phys. **45** (1974) 4288–94.

[17] O. D. Grace, R. R. Goodman: Circumferential waves on solid cyliners. J. Acoust. Soc. Am. **39** (1966) 173–174.

[18] L. M. Brekhovskikh: Surface waves confined to the curvature of the boundary in solid. Sov. Phys. Acoust. **13** (1968) 462–472.

[19] J. Cerv: Dispersion of elastic waves and Rayleigh-type waves in a thin disc. Acta Tech. CSAV **89** (1988) 89–99.

[20] G. Liu, J. Qu: Guided circumferential waves in a circular annulus. Journal of Applied Mechanics, Transactions ASME **65** (1998) 424–430.

[21] G. Liu, J. Qu: Transient wave propagation in a circular annulus subjected to transient excitation on its outer surface. Journal Acoustical Society of America **104** (1998) 1210–1220.

[22] C. Valle, J. Qu, L. J. Jacobs: Guided circumferential waves in layered cylinders. Int. J. Eng. Sci. **37** (1999) 1369–1387.

[23] C. He, L. Li, B. Wu: Guided circumferential waves in hollow cylinders. Chinese Journal of Mechanical Engineering **40** (2004) 7–12.

[24] S. Towfighi, T. Kundu, M. Ehsani: Elastic wave propagation in circumferential direction in anisotripic cylindrical curved plates. Journal of Applied Mechanics **69** (2002) 283–291.

[25] J. Yu, B. Wu, C. He: Guided circumferential waves in orthotropic cylindrical curved plate and the mode conversion by the end-reflection. Applied Acoustics **68** (2007) 594–602.

[26] J. E. Lefebvre, V. Zhang, J. Gazalet, T. Gryba: Legendre polynomial approach for modeling free-ultrasonic waves in multilayered plates. Journal of Applied Physics **85** (1999) 3419–3427.